RSC Advances

ROYAL SOCIETY OF CHEMISTRY

www.rsc.org/advances

Graphical Abstract

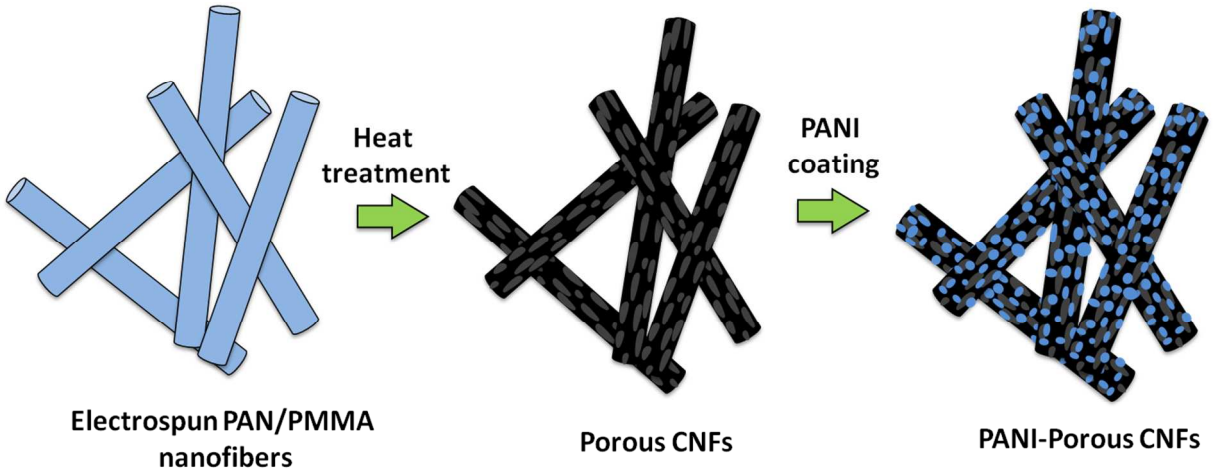

Polyaniline-porous carbon nanofiber composites were introduced for use as flexible, binder-less electrodes for high-performance supercapacitors.

Free-standing polyaniline-porous carbon nanofiber electrodes for symmetric and asymmetric supercapacitors

Mahmut Dirican[1,2], Meltem Yanilmaz[1], and Xiangwu Zhang[1]*

[1] Fiber and Polymer Science Program, Department of Textile Engineering, Chemistry and Science, North Carolina State University, Raleigh, NC 27695-8301, USA

[2] Nano-Science and Nano-Engineering Program, Graduate School of Science, Engineering and Technology, Istanbul Technical University, Istanbul, 34469, TURKEY

***Corresponding author:** Xiangwu Zhang,

Tel: 919-515-6547; Fax: 919-515-6532; E-mail: xiangwu_zhang@ncsu.edu

Abstract

Polyaniline (PANI)-porous carbon nanofiber (PCNF) composites were generated by in-situ polymerization of aniline on PCNFs for use as flexible, binder-less electrodes for high-performance supercapacitors. The effect of polymerization time on the electrode performance was studied by using symmetric cell configuration. Because of the high faradic current and good charge transfer between PCNFs and PANI, a maximum specific capacitance of 296 F/g and excellent rate performance were achieved for PANI-PCNF electrodes. PANI-PCNF electrodes also showed good capacitance retention (98%) after 1000 charge-discharge cycles. Furthermore, an asymmetric cell was successfully fabricated by using PANI-PCNF as the positive electrode and PCNFs as the negative electrode. Energy density and power density were improved significantly by using the asymmetric cell configuration. The resultant PANI-PCNF//PCNF asymmetric supercapacitor exhibited an energy density of 353 Wh/kg with the power density of 609 W/kg at a current density of 1 A/g.

Keywords: Supercapacitor; Porous carbon nanofiber; Polyaniline; Energy density; Power density

Introduction

Supercapacitors have attracted great attention for many applications such as digital communication devices, flexible and wearable electronics and electric vehicles due to their high power densities, fast charging-discharging processes and long cycle life.[1-3] In carbon based supercapacitors, electric double layer capacitance is formed when positive and negative ionic charges within the electrolyte accumulate on the electrode surfaces. During charging, the negative electrode attracts cations while anions accommodate on the positive electrode. Double layer capacitance is determined by the amount of interfacial area between the electrolyte and the electrode. Therefore, high capacitance and energy densities can be obtained by using carbon materials with large surface area and porosity.[4] However, the double layer capacitance resulted by the reversible adsorption of electrolyte ions onto the electrode surfaces is not high enough for many applications. To address this problem, faradic pseudo capacitance has been developed by using conductive polymers and/or metal oxides. These active species can be oxidized or reduced reversibly and such redox reactions provide high pseudo capacitance at the interface of the electroactive species.[4-6]

Among various conductive polymers, polyaniline (PANI), polypyrrole (PPy) and poly(3,4-ethylene-dioxythiophene) (PEDOT) have been found to be suitable for use in supercapacitor applications. They not only show large pseudo capacitance due to their oxidation-reduction properties but also have high surface area and good electrical conductivity.[4, 7] Low cost, ease synthesis and high charge density are some other advantages of these conductive polymers.[8, 9]However, most conductive polymers are mechanical instable due to their brittle nature and have poor processability because of their low solubility in common solvents.[10, 11] In

addition, when used as supercapacitor electrode materials, conductive polymers often show poor cycling performance owing to their large volume change during cycling.[2, 12] One possible approach to solve these problems is to combine conductive polymers with high-surface area carbons to create composite electrodes that combine the advantages of both materials while overcoming their disadvantages.

In this work, PANI-coated porous carbon nanofiber (PCNF) composites were prepared by chemical polymerization of aniline on electrospun PCNFs for use as high-performance supercapacitor electrodes. The resultant PANI-PCNF composite electrodes combine the large pseudo capacitance of the conducting PANI polymer with the fast charging/discharging double-layer capacitance of PCNFs. Redox reactions require large interfacial area between the electrode and the electrolyte. Up to now, studies have been reported on the preparation of high-surface area PANI-carbon composites.[4, 13-15] However, most of these reported PANI-carbon composites were prepared in the powder form and they needed polymer binders to prepare useful electrodes. It has been well established that the use of polymer binders could not only increase the total weight of electrodes but also hinder their performance in supercapacitors.[16] Electrospun PCNF sheets have large surface area and high porosity, and hence they can serve as the ideal scaffold for PANI loading.[17, 18] The resultant PANI-PCNF composites are highly conductive and free-standing, and they can be used directly as binder-free electrodes in supercapacitors. For fabrication of PANI-PCNF electrodes, PCNFs were first produced by electrospinning of a polyacrylonitrile (PAN)/polymethylmethacrylate (PMMA) blend solution, followed by heat treatment. During the heat treatment, PAN was pyrolyzed to form the carbon matrix while PMMA was thermally decomposed to create a porous structure for increasing the surface area. Aniline was then chemically polymerized on the surface of PCNFs. The performance of PANI-

PCNF electrodes was investigated by means of fabricating both the symmetric and asymmetric cells. Results showed that the as-prepared PANI-PCNF electrodes possessed high capacitance with excellent cycling stability. PANI-PCNF//PCNF asymmetric supercapacitors demonstrated an energy density of 353 Wh/kg with the power density of 609 W/kg at a current density of 1 A/g. Energy density and power density of PANI-PCNF/PANI-PCNF symmetric supercapacitors at the same current density were determined as 46 Wh/kg and 361 W/kg, respectively. Therefore, free-standing and binder-free PANI-PCNF composites are promising electrode candidate for supercapacitor applications.

2. Experimental

2.1 Chemicals

Aniline, ammonium persulfate (APS), sulfuric acid (H_2SO_4), polymethylmethacrylate (PMMA, M_w = 130000) and N,N-dimethyl formamide (DMF) were purchased from Sigma Aldrich. Polyacrylonitrile (PAN, M_w = 150000) was supplied from Pfaltz& Bauer Inc. All chemicals were used without further purification.

2.2 Preparation of PCNFs

PAN/PMMA solution (8 wt. %) was prepared by dissolving PAN and PMMA with a PAN-to-PMMA mass ratio of 7/3 into DMF at 60 ^oC under mechanical stirring for 24 h. The as-prepared PAN/PMMA solution was then electrospun into nanofibers with a flow rate of 0.75 ml/h, a voltage of 16 kV, and a tip-to-collector distance of 15 cm. Electrospun PAN/PMMA

nanofibers were stabilized in air environment at 280 ^{o}C for 5.5 h with a heating rate of 5 ^{o}C/min and then carbonized at 700 ^{o}C for 2 h in argon atmosphere with a heating rate of 2 ^{o}C/min, during which PAN was pyrolyzed to carbon and PMMA was thermally decomposed to create a porous structure in the carbon matrix. As-prepared PCNFs formed free-standing sheets, which were used as the substrate to polymerize aniline.

2.3 Preparation of PANI-PCNF electrodes

PANI-PCNF electrodes were prepared by *in-situ* chemical polymerization of aniline on the surface of PCNFs. Prior to polymerization, PCNF sheets were first treated in 25% HCI for 20 min. The pre-treated PCNF sheets were then immersed into 0.1 M aniline/1 M HCI solution, followed by the addition of 0.1 M APS/1 M HCI solution dropwise. The polymerization temperature was kept at about 0 ^{o}C while the polymerization time was varied from 6 h, 12 h to 24 h to investigate its effect on electrochemical performance. The as-prepared PANI-PCNF sheets were free-standing and they were directly used as electrodes after being washed for several times with deionized water and ethanol.

2.4 Structure Characterization

The morphology of PANI-PCNF electrodes was studied by using a JEOL JSM-6400F field-emission scanning electron microscope (FESEM) and transmission electron microscope (TEM, JEOL JEM-2000FX). The structure of PANI-PCNF electrodes was also investigated by Fourier transform infrared spectroscopy (FTIR, Nicolet Nexus 470).

2.5 Performance evaluation

The electrochemical properties of the supercapacitor electrodes were studied by assembling of symmetric and asymmetric Swagelok cells using two-electrode configuration. For symmetric cells, the same material was used on both sides as the positive and negative electrodes. Asymmetric supercapacitor cells were assembled by using PANI-PCNF as the positive electrode and PCNFs as the negative electrode, respectively. Glass microfiber filters (Whatman) was used as the separator and was soaked in 1 M H_2SO_4 electrolyte solution before cell assembly. The reproducibility of the testing results was assessed by conducting all measurements on at least five samples for each composite. Specific capacitance and energy density results of the electrodes were reported with error bars, on which mean values and standard deviations of the testing experiments were represented. For most samples, the standard deviations ranged from 7 to 15 F/g for specific capacitance values and 0.5 to 1.1 Wh/kg for the energy density values.

Resistance of the electrodes were measured by electrochemical impedance spectroscopy (EIS) over a frequency range of 100 kHz to 0.1 Hz with AC amplitude of 5 mV at room temperature using Reference 600 Potentiostat/Galvanostat/ZRA (GAMRY) and resistance results were determined based on the values on the Z' axis of the Nyquist plots in "Ω" unit. Cycling voltammetry was used to analyze the electrochemical behavior of the PANI-PCNF electrodes at different scan rates.

The electrochemical performance was investigated by carrying out galvanostatic charge-discharge experiments at constant current density of 1A/g with cut-off potentials of -0.4 and 0.6 V using Arbin automatic battery cycler. The specific capacitance (C_s) of the electrodes was calculated by using the following equation:

$$Specific\ capacitance\ (C_s) = \frac{2 \times I \times t}{W \times \Delta E} \quad (1)$$

where I is the discharge current, t the discharge time, W the mass of the electrode, and ΔE the voltage difference in discharge.[19,20] The rate performance was measured using the same instrument at current densities of 1, 2, 3, 4, and 5 A/g.

The average energy density ($E_{density}$) and power density ($P_{density}$) of the electrodes for both asymmetric and symmetric cell configurations were calculated according to equations (2) and (3), respectively.

$$E_{density} = \frac{1}{2} C V_{max}^2 \quad (2)$$

and

$$P_{density} = \frac{E_{density}}{\Delta_t} \quad (3)$$

where C is the total specific capacitance, V_{max} the maximum charging voltage, and Δ_t the discharge time.[19-21]

3. Results and Discussion

3.1 Electrode morphology

PAN/PMMA precursor nanofibers were first prepared by electrospinning, which were then heat-treated to form PCNFs. TEM characterization was employed to demonstrate the porous

structure of PCNFs and the results are shown in Figure 1. The porous structure created by the decomposition of PMMA can be clearly observed on PCNFs in the TEM images.

PANI/PCNF composites were obtained by chemical polymerization of aniline on the surface of PCNFs. Figures 2A, B, and C show the SEM images of PANI-PCNFs prepared using different polymerization times of 6 h, 12 h, and 24 h, respectively. From SEM images of PANI-PCNFs, uniform PANI coating on PCNF sheets was observed due to the strong adhesive force between the PANI chains and PCNF surface. For comparison, PANI film was also synthesized without the presence of PCNFs and its SEM image is shown in Figure 2D. It was seen that the as-synthesized PANI had plate-like structure.

Figure 3 shows TEM images of PANI-PCNFs prepared with a polymerization time of 12 h. TEM images of PANI-PCNFs demonstrated that PCNFs were thoroughly coated by tree bark like PANI layer. Formation of PANI coating on highly-porous interconnected carbon nanostructure led to easy access of liquid electrolyte and fast ion diffusion and migration, which resulted in enhanced electrochemical performance as discussed below.

3.2 Structure analysis

Figure 4 shows FTIR spectra of PCNFs and PANI-PCNFs prepared with different polymerization times. For comparison, the FTIR spectrum of PANI film synthesized without the presence of PCNFs is also shown. PCNFs presented two characteristic peaks at around 1280 cm^{-1} and 1590 cm^{-1}, which could be ascribed to C-C and C=C stretching bonds, respectively. PANI showed more characteristic peaks, which can be associated with C-C stretching mode vibrational band of the quinoid structure at around 1483 cm^{-1}, C=C stretching mode vibrational band of the benzonoid structure at 1567 cm^{-1}, C-H stretching from aromatic conjugation at

around 1246 and 1300 cm^{-1}, and C-N stretching of the secondary aromatic amine, aromatic C-H in plane bending and out of plane C-H bending vibration at 1293, 1119 and 795 cm^{-1}, respectively. [2] From Figure 4, it was also seen that the characteristic peaks corresponding to the PANI structure were presented in the FTIR spectra of PANI-PCNFs prepared with different polymerization times of 6 h, 12 h and 24 h. On the other hand, the characteristic peaks of PCNFs couldn't be found on PANI-PCNFs, indicating that the surface of PCNFs was completely covered by PANI after the polymerization of aniline.

3.3 Electrochemical characteristics of PANI-PCNF electrodes

Cycling voltammetry (CV) was used to analyze the electrochemical behavior of PCNF and PANI-PCNF electrodes in 1 M H_2SO_4 electrolyte with a scan rate of 5 mV/s, and the results are shown in Figure 5. The CV curve of PCNF electrodes demonstrated the typical double-layer capacitance characteristic, i.e., the rectangular-like shape. On the other hand, redox peak couples were observed from CV curves of PANI-PCNF electrodes. PANI-PCNF electrode with 12 h polymerization time showed an oxidation peak at around 0.15 V, which was attributed to the oxidation of PANI. In addition, one well-defined reduction peak at around 0.25 V was observed on the cathodic scan. It must be noted that PANI-PCNF electrodes with 6 and 24 h polymerization times did not show apparent oxidation peaks, but exhibited reduction peaks at around 0.15 V. Similar trend was reported by Gupta et al. for polyaniline/single-wall carbon nanotube (PANI/SWCNT) composites electrodes.[22] On the CV curves, they did not observe apparent redox peaks for PANI/SWCNT composite electrodes in 1 M H_2SO_4 electrolyte solution and claimed that results implied the stability of the electrolyte. However, more work is needed to fully understand the mechanism. In addition, from Figure 5, faradic currents caused by the redox

reaction of PANI we observed in the voltammograms of PANI-PCNF electrodes, which indicated that these electrodes had higher capacitances than the PCNF electrode. Compared with the PCNF electrode, PANI-PCNF electrodes showed significantly higher background currents in the voltammograms. In addition, an increase in current density can be observed by increasing polymerization time from 6 h to 12 h simply because more PANI was formed with longer polymerization time. However, there was a slight decrease in the maximum current when the polymerization time was 24 h. Figure 6 shows the CV curves for the PCNF and PANI-PCNF electrodes at different scan rates ranging from 5 to 400 mV/s. For all four electrodes, the current densities increased with increase in scan rate, indicating their good rate capability. However, the slight decrease in the maximum current was observed for PANI-PCNF electrode with 24 h polymerization time. This unusual behavior may be attributed to the self-agglomeration of coated PANI polymer over the electrode surface. With a polymerization time of 24 h, the self-agglomeration of coated PANI might hinder the diffusion of the electrolyte into the electrode, an as a result, some of the PANI chains might not participate in the redox reactions. This could cause the decrease of the maximum current.

Electrochemical information including electrolyte resistance and charge transfer resistance was also obtained using EIS. Nyquist plots of PCNF and PANI-PCNF electrodes are shown in Figure 7. All curves exhibited a semi-circle in the high frequency region and a straight line in the low frequency region, indicating a capacitive behavior. The high frequency semi-circle was attributed to the charge transfer process at the electrode/electrolyte interface. The straight line in the low frequency region represented a diffusion-limiting step in the electrochemical process.[23] Charge transfer resistance (*Rct*) of the PCNF electrode was 13 Ω, which decreased to 8 Ω, 6 Ω and 10 Ω, respectively, for PANI-PCNF electrodes with 6 h, 12 h,

and 24 h polymerization times. The PANI-PCNF electrode with 12 h polymerization time gave the lowest resistance because of the excellent charge transfer ability between PANI and PCNF. Thereafter, the resistance increased from 6 to 10 Ω, which was attributed to the decreased electrolyte ion diffusion into the electrode material caused by the increased self-agglomeration of coated PANI polymer with longer coating time. Similar trend was observed by Gupta, et al. for PANI/carbon nanotube composites.[22]

There are other groups who reported similar EIS results for conducting polymer-carbon based composites. For example, Zhang and coworker reported a *Rct* value that was lower than 13 ohms for graphene/polypyrrole composite electrodes.[24] In their work, the R*ct* value for the graphene/polypyrrole composite electrode was only around 4 Ω with 1 M H_2SO_4 electrolyte solution. In addition, they also found that electrolyte resistance of their 1 M H_2SO_4 electrolyte solution was very close to zero, which was similar to our result.

3.4 Charge-discharge cycling and C-rate performance of PANI-PCNF electrodes

Typical charge-discharge curves of PANI-PCNF electrodes at 1 A/g between -0.4 and 0.6 V are shown in Figure 8. The specific capacitance of the PCNF electrode was 127 F/g, which increased to 272, 296, and 217 F/g, respectively, for PANI-PCNF electrodes prepared with polymerization times of 6 h, 12 h, and 24 h. PANI-PCNF electrodes had higher capacitances than the PCNF electrode due to the contribution of faradic pseudocapacitance of PANI. In addition, the discharge curves of PANI-PCNF electrodes were almost linear, indicating that they have good capacitive behavior.

From Figure 8, it was also seen that the specific capacitance of PANI-PCNF electrodes was the highest (296 F/g) when the polymerization time used was 12 h. For pseudocapacitors,

the energy-storage mechanism is based on fast faradic redox reactions that occur at the interface between the active material and the electrolyte. The high capacitance of the PANI-PCNF electrode (polymerization time = 12 h) could be explained by the high amount of PANI coating and the decreased charge transfer resistance of the electrode as demonstrated by impedance spectroscopy (Figure 7). However, when the polymerization time was further increased from 12 h to 24 h, slight decrease in specific capacitance was observed. This capacitance decrease of the PANI-PCNF electrode (polymerization time = 24 h) could be attributed to its higher diffusion resistance, as shown in Figure 7. Because beyond certain coating thickness, the electrolyte might not be able to diffuse into the electrode effectively and not all the PANI chains participated in redox reactions. This result agrees with previous studies by Zhang, et al. and Gupta, et al. on fabrication of conductive polymer-coated graphene and carbon nanotube composite electrodes.[22, 24]

Supercapacitor electrodes must have high capacitances at high current densities, especially for high power applications. Specific capacitances of PCNF and PANI-PCNF electrodes at different current densities are shown in Figure 9. It was seen that for all four electrodes, the increase in current density led to decrease in specific capacitance due to the electrode polarization. For example, the PCNF electrode had a capacitance of 127 F/g at 1 A/g, which decreased slightly to 105 F/g at 5 A/g. Capacitances of PANI-PCNF electrodes prepared with polymerization times of 6, 12, and 24 h were 272, 296 and 217 F/g at 1 A/g and 220, 238 and 164 F/g at 5 A/g, respectively. Among all electrodes, the PANI-PCNF electrode with the polymerization time of 12 h had the highest specific capacitance at all current densities due to its low charge transfer resistance. The relatively small decrease in specific capacitance with

increasing current density indicated the fast ion diffusion in these electrodes and demonstrated their good rate capability.

The cycling performance of PCNF and PANI-PCNF electrodes was evaluated by galvanostatic charge-discharging at a constant current of 1 A/g in 1 M H_2SO_4 electrolyte for 1000 cycles, and the results are shown in Figure 10. For comparison, the cycling performance of PANI electrode is also shown. It was seen that the PCNF electrode had the highest capacitance retention of 99% in the first 1000 cycles. The low capacitance loss of PCNF electrode was due to the high stability of the carbon structure. On the other hand, the PANI electrode exhibited 56% capacitance loss in the first 1000 cycles. This large capacitance loss was caused by the repeated swelling and shrinking of the PANI polymer during cycling, leading to the damaged electrode structure.[25] Coating PANI onto the surface of PCNFs could utilize the stable carbon structure to accommodate the volume change and mechanical deformation of PANI polymer during cycling. As shown in Figure 10, the resultant PANI-PCNF electrodes had improved capacitance retentions of 95, 98 and 92% in the first 1000 cycles, respectively, for 6, 12 and 24 h polymerization times. Among these three samples, the PANI-PCNF electrode with the polymerization time of 12 h had the highest capacitance retention. The PANI-PCNF electrode with 24 h polymerization time showed larger capacitance loss compared to other PANI-PCNF electrodes. This result agrees with a previous study by Cheng et al. on using PANI-coated electro-etched carbon fiber cloth as the supercapacitor electrode.[8] In that study, higher capacitance loss was observed for thick PANI layers because they tended to fall apart from the carbon substrate during prolonged cycling.

3.5 Energy and power densities of PANI-PCNF based symmetric supercapacitors

Ragone plots, which map the energy density and power density, of PCNF/PCNF, PANI/PANI, and PANI-PCNF/PANI-PCNF symmetric cells by varying current densities (1, 2, 3, 4, and 5 A/g) are demonstrated in Figure 11. The PANI-PCNF electrodes were prepared using the polymerization time of 12 h. From Figure 11, it is seen that the PCNF/PCNF symmetric cell showed a relatively low energy density of 12 Wh/kg with a power density of 180 W/kg at a current density of 1 A/g. On the other hand, both PANI/PANI and PANI-PCNF/PANI-PCNF cells exhibited higher energy density of around 23 Wh/kg with a power density of 180 W/kg at a current density of 1 A/g. At a higher current density of 5 A/g, the energy densities of PCNF/PCNF, PANI/PANI, and PANI-PCNF/PANI-PCNF symmetric cells decreased to 10 Wh/kg, 13 Wh/kg, and 18 Wh/kg, respectively, while their power densities increased to 903 W/kg, 908 W/kg, and 851 W/kg. Therefore, among all three cells, PANI-PCNF/PANI-PCNF symmetric cells have the greatest energy density mainly due to the high capacitance of PANI-PCNF electrodes.

3.6 Energy and power densities of PANI-PCNF based asymmetric supercapacitors

There are two important approaches to improve the energy density of supercapacitors. The first one is to increase the capacitance of electrodes and the second one is to use an asymmetric supercapacitor design.[26] As discussed in the previous section, PANI-PCNF/PANI-PCNF symmetric cells had higher energy density than PCNF/PCNF and PANI/PANI symmetric cells because of the high capacitance of PANI-PCNF electrodes. In this work, asymmetric cells were also fabricated and tested by using PANI and PANI-PCNF electrodes as the cathode and PCNF electrode as the anode over a potential range of -0.5 to 1.6 V. Typical charge-discharge curves of PANI-PCNF//PCNF and PANI//PCNF asymmetric cells at 1 A/g are shown in Figure

12. It is seen that the specific capacitance of PANI-PCNF//PCNF asymmetric cells was much higher than that of PANI//PCNF asymmetric cells. Specific capacitances of PANI-PCNF//PCNF and PANI//PCNF asymmetric cells at different current densities are shown in Figure 13. PANI-PCNF//PCNF asymmetric cells provided higher specific capacitance than PANI//PCNF asymmetric cells at all current densities. Relatively small decrease in specific capacitance with increasing current density was also observed for PANI-PCNF//PCNF asymmetric cells. Figure 14 represents the Ragone plots of PANI-PCNF//PCNF and PANI//PCNF asymmetric cells by varying current densities (1, 2, 3, 4, and 5 A/g). By comparison of Figures 11 and 14, it was seen that both energy density and power density were improved by using the asymmetric cell configuration. For the asymmetric configuration, the energy density and power density of PANI-PCNF//PCNF cells approached 177 Wh/kg and 304 W/kg, respectively, at a current density of 1 A/g. Even at a high current density of 5 A/g, the energy density still remained at 118 Wh/kg with the power density increased to 1524 W/kg, indicating that large power range could be obtained while maintaining high energy density. In contrast, PANI//PCNF asymmetric cells delivered much lower energy density of 86 Wh/kg and comparable power density of 319 W/kg at a current density of 1 A/g. At a current density of 5 A/g, the energy density of PANI//PCNF asymmetric cells reduced to 21 Wh/kg although the power density increased to 1583 W/kg.

To sum up, we introduced conductive polymer (PANI) onto high-surface area porous carbon nanofibers (PCNF) to create composite electrodes that combine the advantages of both materials while overcoming their disadvantages. Different studies have been reported on the preparation of high-surface area conductive polymer-carbon composites, but most of these composites were prepared in the powder form and they needed polymer binders to prepare useful electrodes. For example, Zhang, et al. and Gupta, et al. prepared polypyrrole/graphene composite

and polyaniline/carbon nanotube composite electrodes, respectively, using polyvinylidene fluoride as the binder.[22, 24] During the process, they prepared slurries by mixing their active materials with polyvinylidene fluoride binder and coated them onto the current collector. Even though, they reported reasonable specific capacitance values, which were calculated based on the mass of active material alone, inevitably the energy densities of the final electrodes would be lower than those of binder-free electrodes. The use of an inactive polymer binder could not only increase the total mass of electrodes but also hinder their performance in supercapacitors. However, the PANI-PCNF composite electrodes introduced in this study are highly conductive and free-standing, and they can be used directly as binder-free electrodes in supercapacitors. Results demonstrated that these PANI-PCNF composites are promising supercapacitor electrode candidate and PANI-PCNF based asymmetric cells can achieve high energy and power densities simultaneously.

4. Conclusion

PANI-PCNF electrodes were prepared by chemical polymerization of aniline on electrospun porous carbon nanofibers for use in supercapacitors. Morphology and chemical structure of the electrodes were analyzed by using SEM, TEM and FTIR spectroscopy. The effect of polymerization time on the electrode capacitance was studied by using symmetric cell configuration. Cycling voltammograms and EIS were used to investigate the electrochemical properties of PANI-PCNF electrodes. Galvanostatic charge-discharge testing was used to show the contribution of PANI to overall capacitance of the electrodes. Results showed that the PANI-PCNF electrode prepared with the polymerization time was 12 h exhibited the highest specific

capacitance of 296 F/g at 1A/g in 1 M H_2SO_4 electrolyte because of the high faradic current and good charge transfer between PCNFs and PANI. Low charge-transfer resistance was also observed for PANI-PCNF electrodes. Excellent rate performance and good capacitance retention (98%) were obtained after 1000 charge-discharge cycles at a current density of 1 A/g. In addition, an asymmetric cell was prepared by using PANI-PCNF as the positive electrode and PCNF as the negative electrode. Energy density and power density were greatly improved by using asymmetric cell configuration. The resultant PANI-PCNF//PCNF asymmetric supercapacitor exhibited an energy density of 353 Wh/kg and a power density of 609 W/kg , respectively, at a current density of 1 A/g, which are determined to be 46 Wh/kg and 361 W/kg for PANI-PCNF/PCNF symmetric supercapacitor. It is, therefore, demonstrated that as-prepared free-standing and binder-free PANI-PCNF composites can be considered as promising electrode candidate for future supercapacitor applications.

References

1. S. Mondal, K. Barai and N. Munichandraiah, *Electrochim. Acta*, 2007, **52**, 3258-3264.
2. L. Li, H. Song, Q. Zhang, J. Yao and X. Chen, *J. Power Sources*, 2009, **187**, 268-274.
3. P. Yu, Y. Li, X. Zhao, L. Wu and Q. Zhang, *Langmuir*, 2014.
4. W.-C. Chen, T.-C. Wen and H. Teng, *Electrochim. Acta*, 2003, **48**, 641-649.
5. H. Lee, H. Kim, M. S. Cho, J. Choi and Y. Lee, *Electrochim. Acta*, 2011, **56**, 7460-7466.
6. J. Xu, K. Wang, S.-Z. Zu, B.-H. Han and Z. Wei, *ACS Nano*, 2010, **4**, 5019-5026.
7. K. Zhang, L. L. Zhang, X. Zhao and J. Wu, *Chem. Mater.*, 2010, **22**, 1392-1401.
8. Q. Cheng, J. Tang, J. Ma, H. Zhang, N. Shinya and L.-C. Qin, *J. Phys. Chem. C*, 2011, **115**, 23584-23590.
9. G. A. Snook, P. Kao and A. S. Best, *J. Power Sources*, 2011, **196**, 1-12.
10. M. Yanilmaz and A. S. Sarac, *Text. Res. J.*, 2014, 0040517513495943.
11. M. Yanilmaz, F. Kalaoglu, H. Karakas and A. S. Sarac, *J. Appl. Polym. Sci.*, 2012, **125**, 4100-4108.
12. D. S. Patil, S. Pawar, R. Devan, S. Mali, M. Gang, Y. Ma, C. Hong, J. Kim and P. Patil, *J. Electroanal. Chem.*, 2014, **724**, 21-28.
13. J. Jang, J. Bae, M. Choi and S.-H. Yoon, *Carbon*, 2005, **43**, 2730-2736.
14. J. J. Cai, L. B. Kong, J. Zhang, Y. C. Luo and L. Kang, *Chin. Chem. Lett.*, 2010, **21**, 1509-1512.
15. W.-x. Liu, N. Liu, H.-h. Song and X.-h. Chen, *New Carbon Mat.*, 2011, **26**, 217-223.
16. C. Kim, K.-S. Yang and W.-J. Lee, *Electrochem. Solid-State Lett.*, 2004, **7**, A397-A399.
17. M. Dirican, M. Yanilmaz, K. Fu, Y. Lu, H. Kizil and X. Zhang, *J. Power Sources*, 2014, **264**, 240-247.
18. Y. Li, G. Xu, Y. Yao, L. Xue, M. Yanilmaz, H. Lee and X. Zhang, *Solid State Ionics*, 2014, **258**, 67-73.
19. W. Chen, Y. He, X. Li, J. Zhou, Z. Zhang, C. Zhao, C. Gong, S. Li, X. Pan and E. Xie, *Nanoscale*, 2013, **5**, 11733-11741.

20. Y. He, W. Chen, J. Zhou, X. Li, P. Tang, Z. Zhang, J. Fu and E. Xie, *ACS Appl. Mater. Interfaces*, 2013, **6**, 210-218.

21. Q. Cheng, J. Tang, N. Shinya and L.-C. Qin, *J. Power Sources*, 2013, **241**, 423-428.

22. V. Gupta and N. Miura, *Electrochim. Acta*, 2006, **52**, 1721-1726.

23. X. Xie and L. Gao, *Carbon*, 2007, **45**, 2365-2373.

24. D. Zhang, X. Zhang, Y. Chen, P. Yu, C. Wang and Y. Ma, *J. Power Sources*, 2011, **196**, 5990-5996.

25. H. Xinping, G. Bo, W. Guibao, W. Jiatong and Z. Chun, *Electrochim. Acta*, 2013, **111**, 210-215.

26. J. Shen, C. Yang, X. Li and G. Wang, *ACS Appl. Mater. Interfaces*, 2013, **5**, 8467-8476.

Table and Figure Captions

Figure 1. TEM images of PCNF (A) and (B).

Figure 2. SEM images of PANI-PCNF electrodes with different polymerization times of 6 h (A), 12 h (B), 24 h (C), and PANI electrode (D).

Figure 3. TEM images of PANI-PCNF electrode with the polymerization time of 12 h (A) and (B).

Figure 4. FTIR spectra of PCNF (A), PANI (B), and PANI-PCNF electrodes with different polymerization times of 6 h (C), 12 h (D) 24 h (F).

Figure 5. Cyclic voltammograms of PCNF and PANI-PCNF electrodes with different polymerization times of 6 h, 12 h and 24 h in 1 M H_2SO_4 at 5 mV/s.

Figure 6. Cyclic voltammograms of PCNF electrode (A), and PANI-PCNF electrodes with the polymerization times of 6 h (B), 12 h (C), and 24 h (D) in 1 M H_2SO_4.

Figure 7. Impedance spectra of PCNF and PANI-PCNF electrodes with different polymerization times of 6 h, 12 h and 24 h.

Figure 8. Galvanostatic charge-discharge curves of PCNF and PANI-PCNF electrodes at a current density of 1 A/g.

Figure 9. Specific capacitances of PCNF, PANI, and PANI-PCNF electrodes with different polymerization times of 6 h, 12 h and 24 h.

Figure 10. Capacitance retention of PCNF, PANI and PANI-PCNF electrodes with different polymerization times of 6 h, 12 h and 24 h.

Figure 11. Ragone plots of PCNF/PCNF, PANI/PANI, and PANI-PCNF/PANI-PCNF symmetric supercapacitors.

Figure 12. Galvanostatic charge-discharge curves of PANI//PCNF and PANI-PCNF//PCNF asymmetric supercapacitors at a current density of 1 A/g.

Figure 13. Specific capacitances of PANI//PCNF and PANI-PCNF//PCNF asymmetric supercapacitors.

Figure 14. Ragone plots of PANI//PCNF, and PANI-PCNF//PCNF asymmetric supercapacitors.

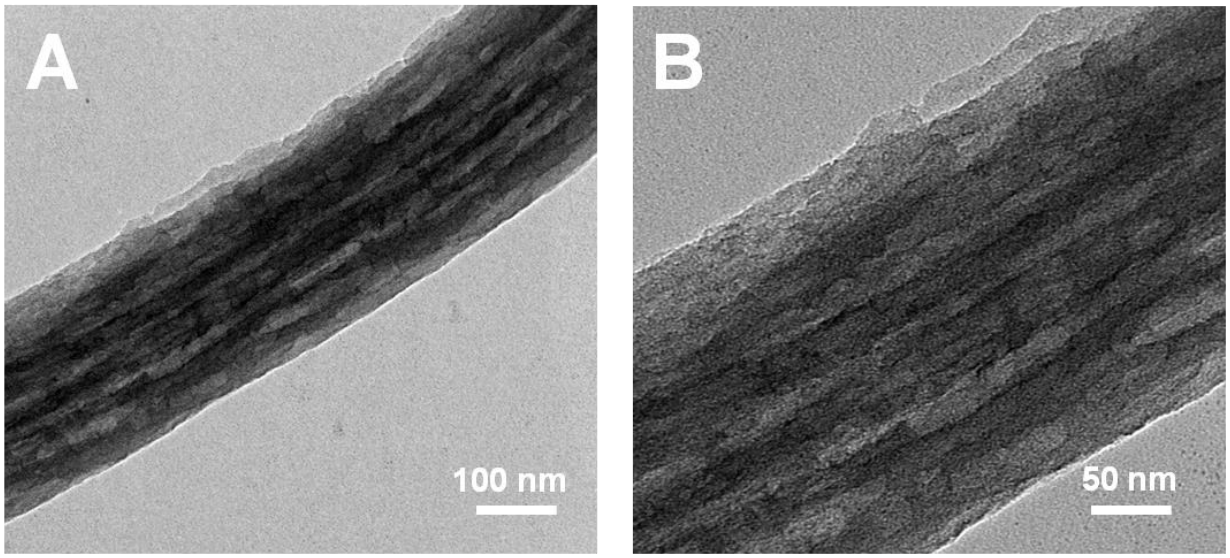

Figure 1. TEM images of PCNFs.

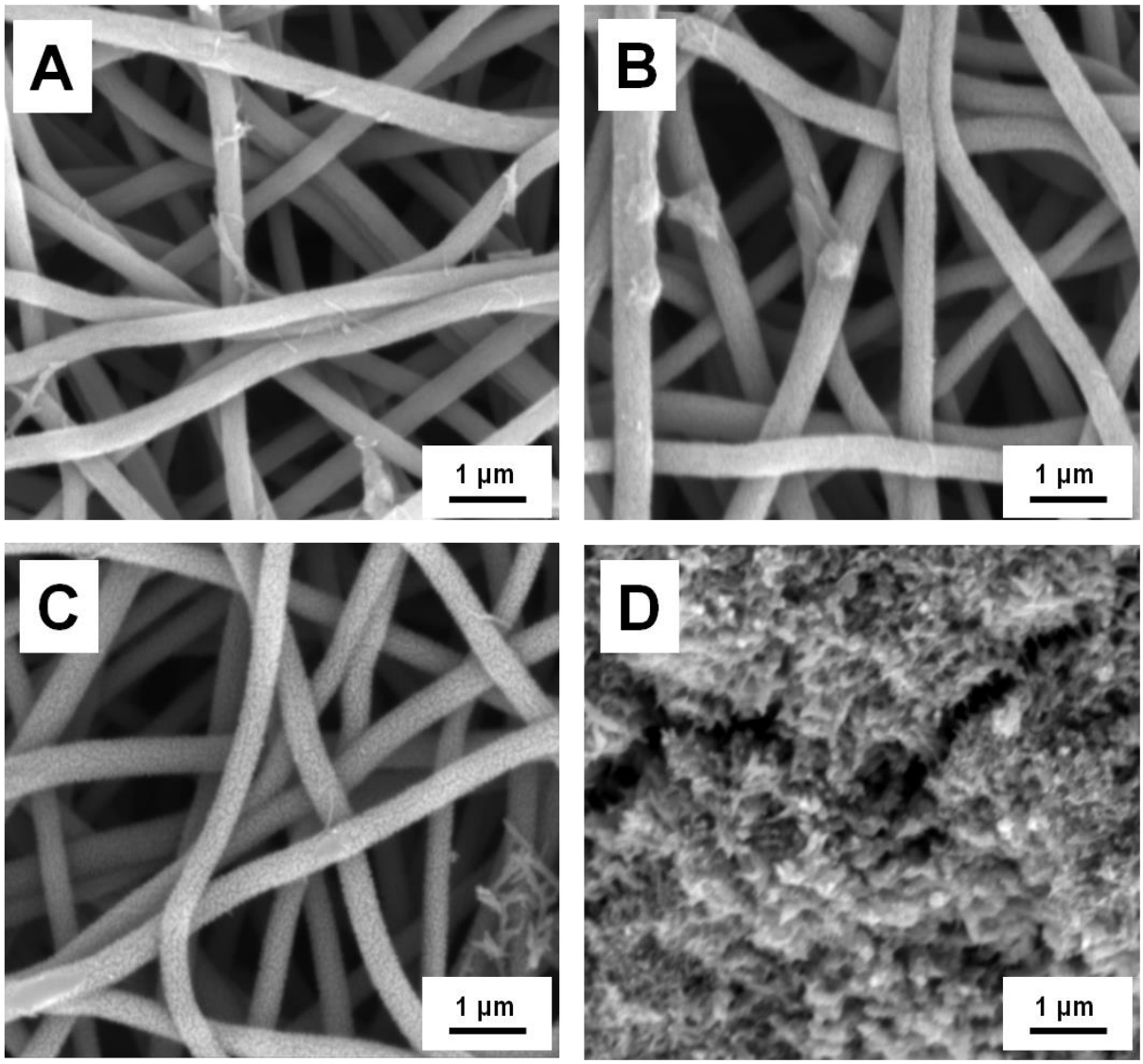

Figure 2. SEM images of PANI-PCNF electrodes with different polymerization times of 6 h (A), 12 h (B), and 24 h (C), and PANI electrode (D).

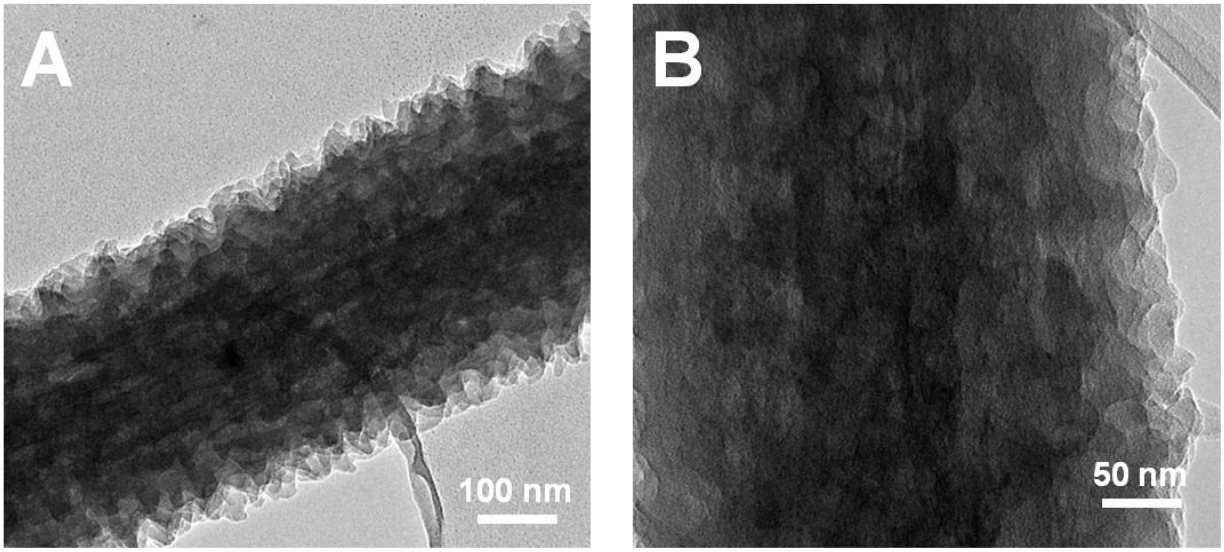

Figure 3. TEM images of PANI-PCNF electrode with the polymerization time of 12 h.

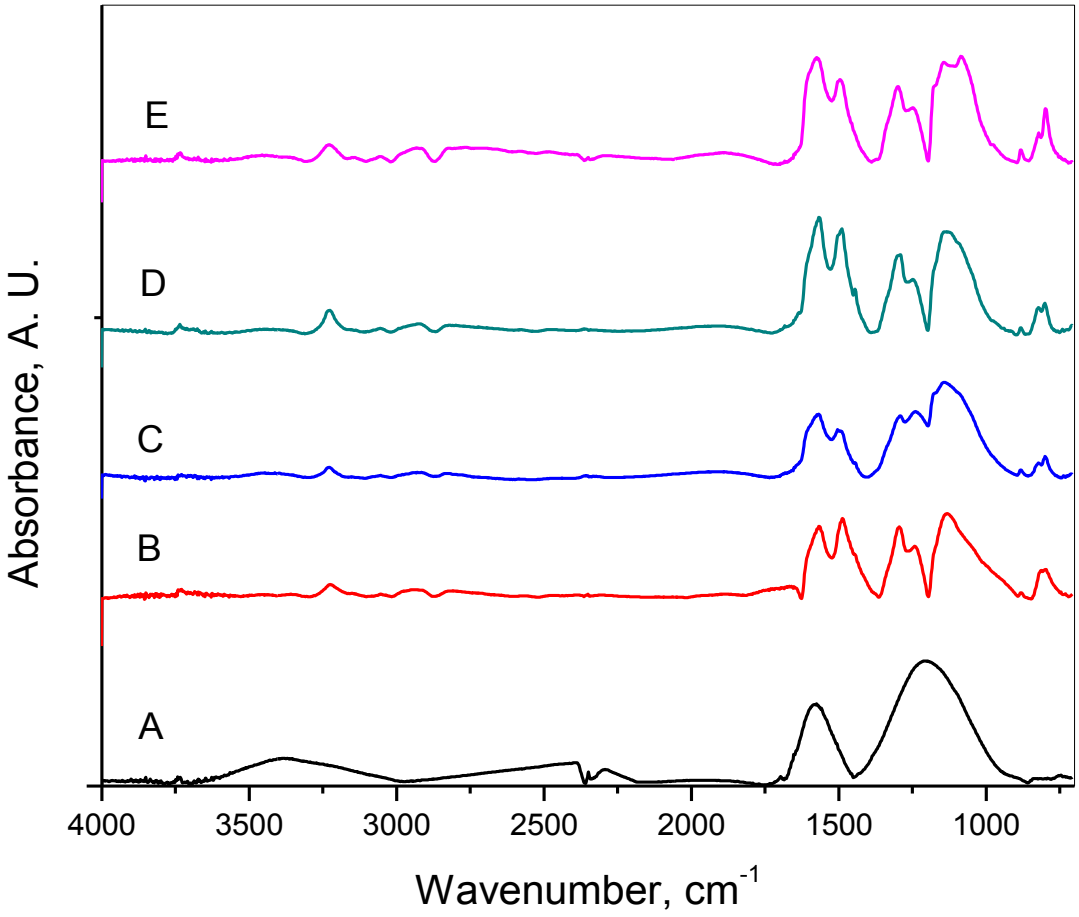

Figure 4. FTIR spectra of PCNF (A), PANI (B), and PANI-PCNF electrodes with different polymerization times of 6 h (C), 12 h (D), and 24 h (F).

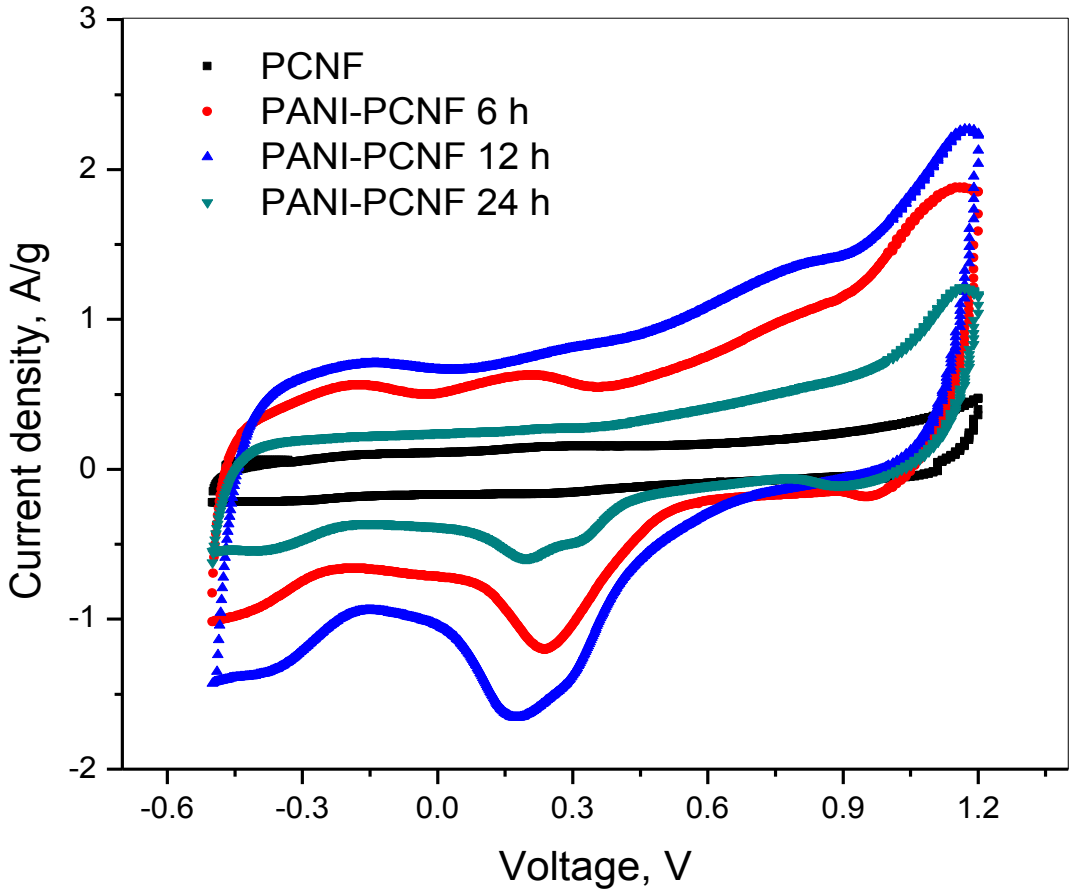

Figure 5. Cyclic voltammograms of PCNF and PANI-PCNF electrodes with different polymerization times of 6 h, 12 h, and 24 h in 1 M H_2SO_4 at 5 mV/s.

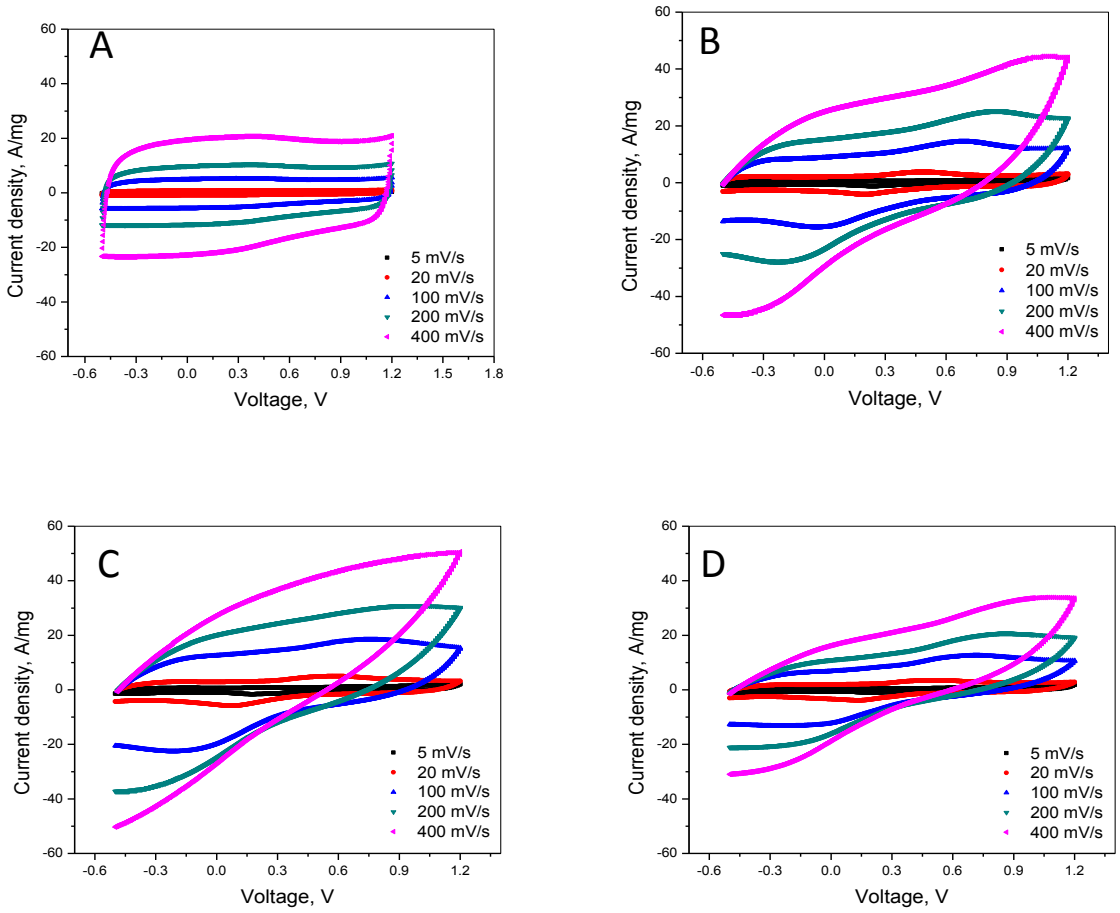

Figure 6. Cyclic voltammograms of PCNF electrode (A), and PANI-PCNF electrodes with different polymerization times of 6 h (B), 12 h (C), and 24 h (D) in 1 M H_2SO_4.

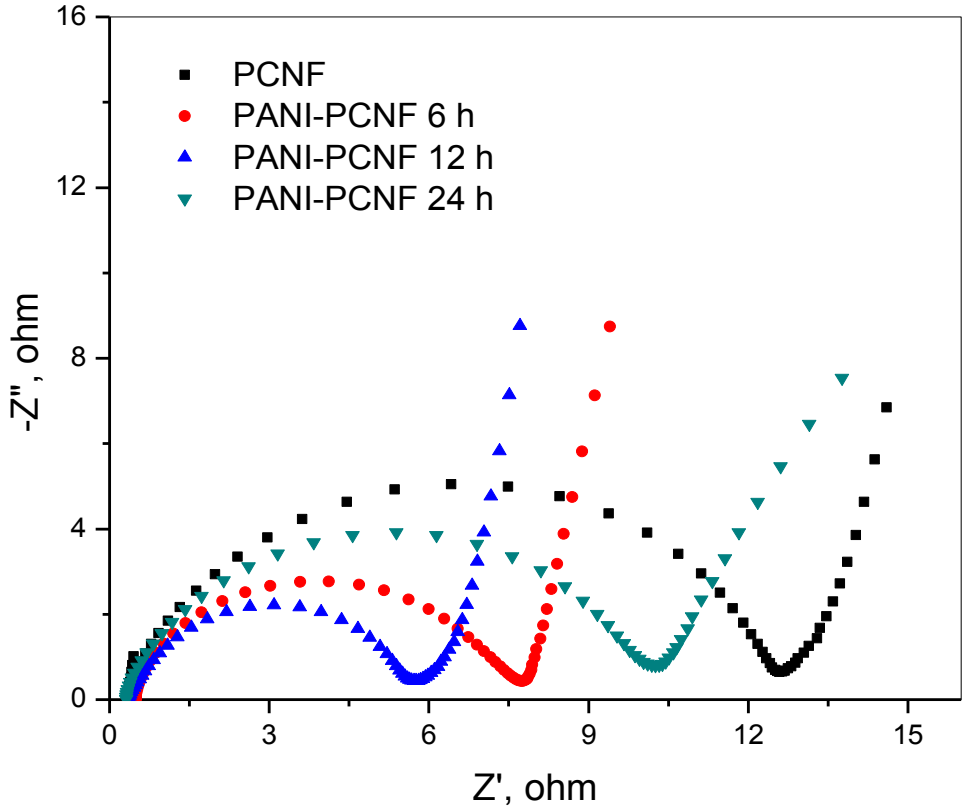

Figure 7. Impedance spectra of PCNF and PANI-PCNF electrodes with different polymerization times of 6 h, 12 h, and 24 h.

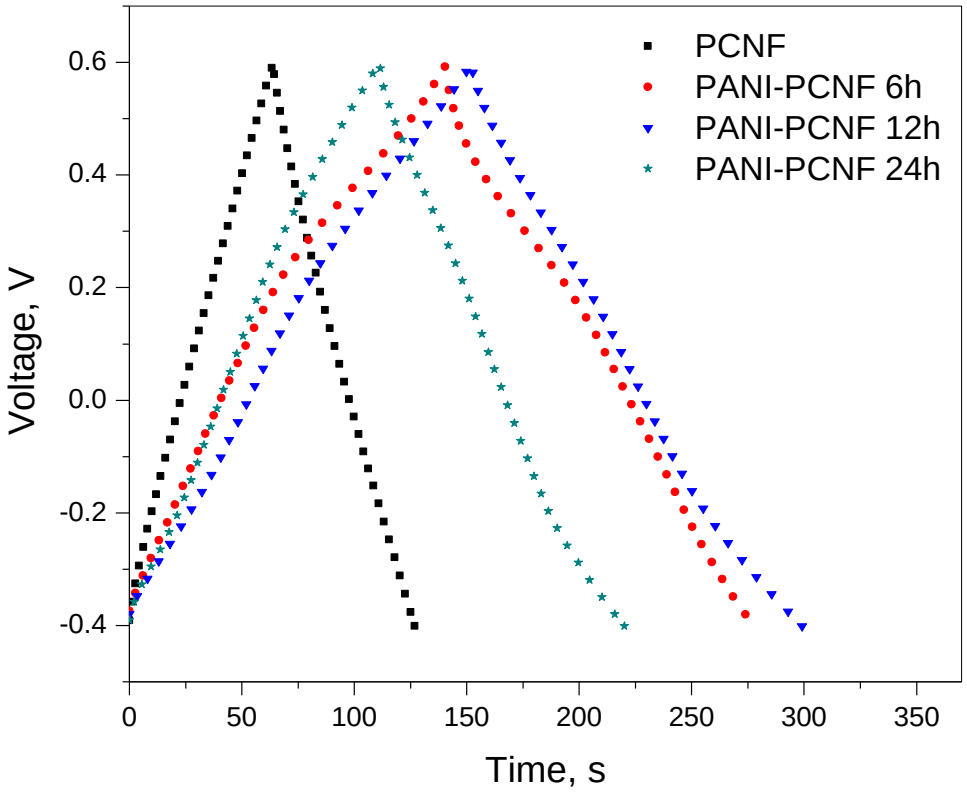

Figure 8. Galvanostatic charge-discharge curves of PCNF and PANI-PCNF electrodes at a current density of 1 A/g.

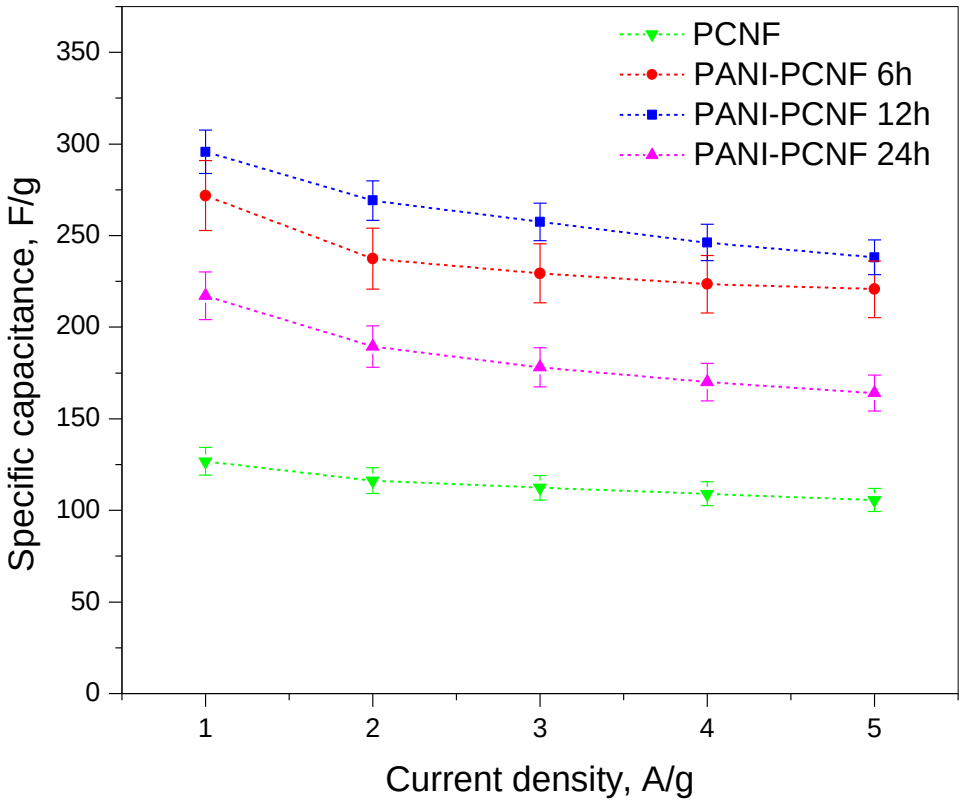

Figure 9. Specific capacitances of PCNF, PANI, and PANI-PCNF electrodes with different polymerization times of 6 h, 12 h, and 24 h.

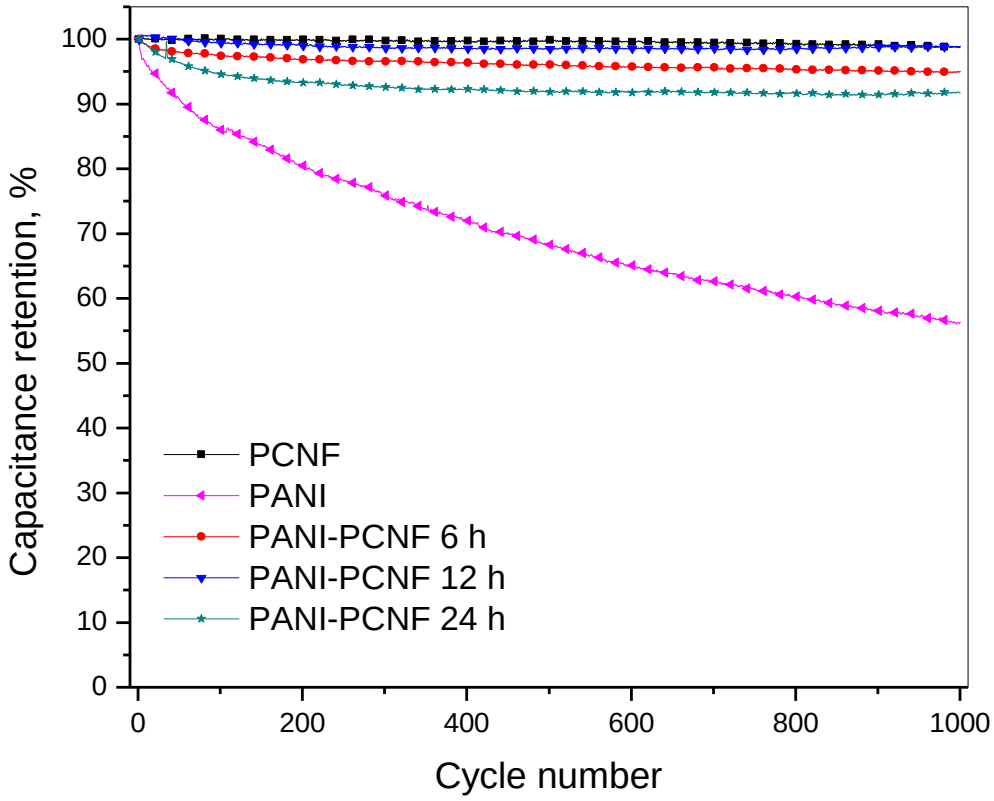

Figure 10. Capacitance retention of PCNF, PANI and PANI-PCNF electrodes with different polymerization times of 6 h, 12 h, and 24 h.

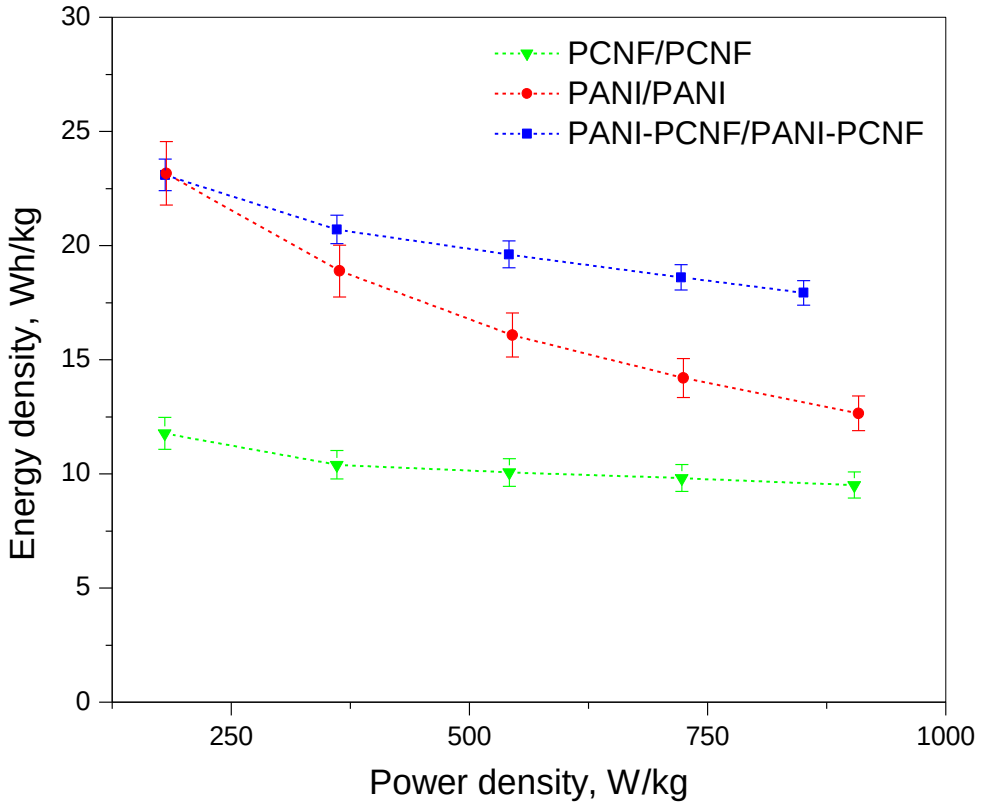

Figure 11. Ragone plots of PCNF/PCNF, PANI/PANI, and PANI-PCNF/PANI-PCNF symmetric supercapacitors.

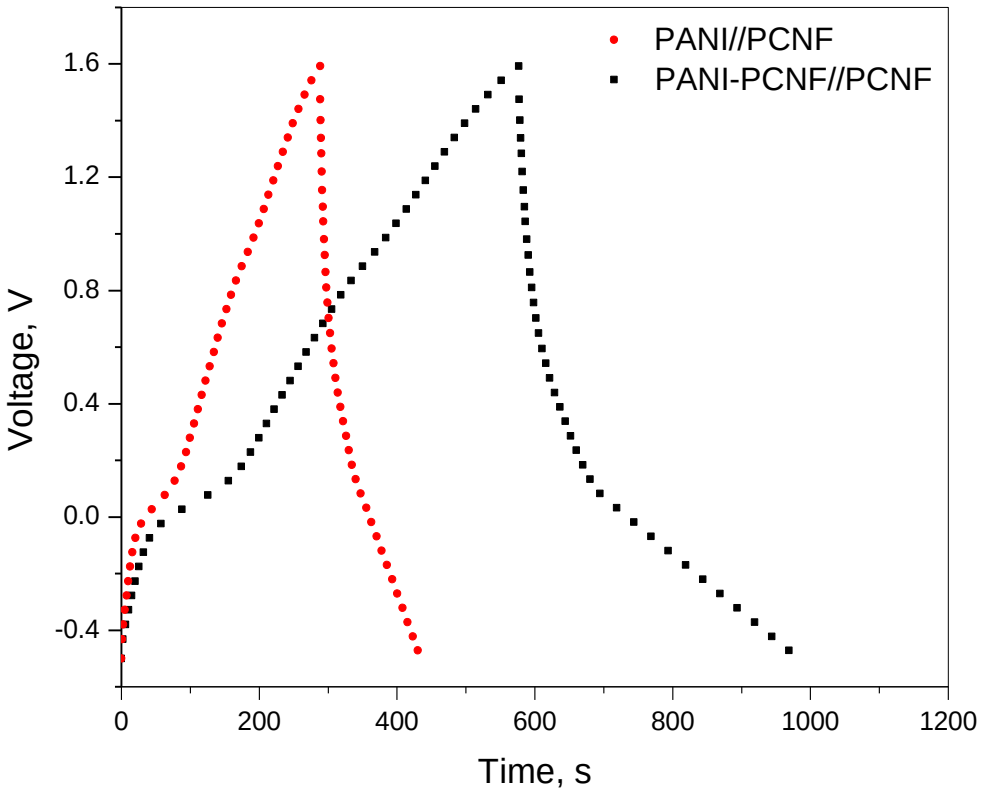

Figure 12. Galvanostatic charge-discharge curves of PANI//PCNF and PANI-PCNF//PCNF asymmetric supercapacitors at a current density of 1 A/g.

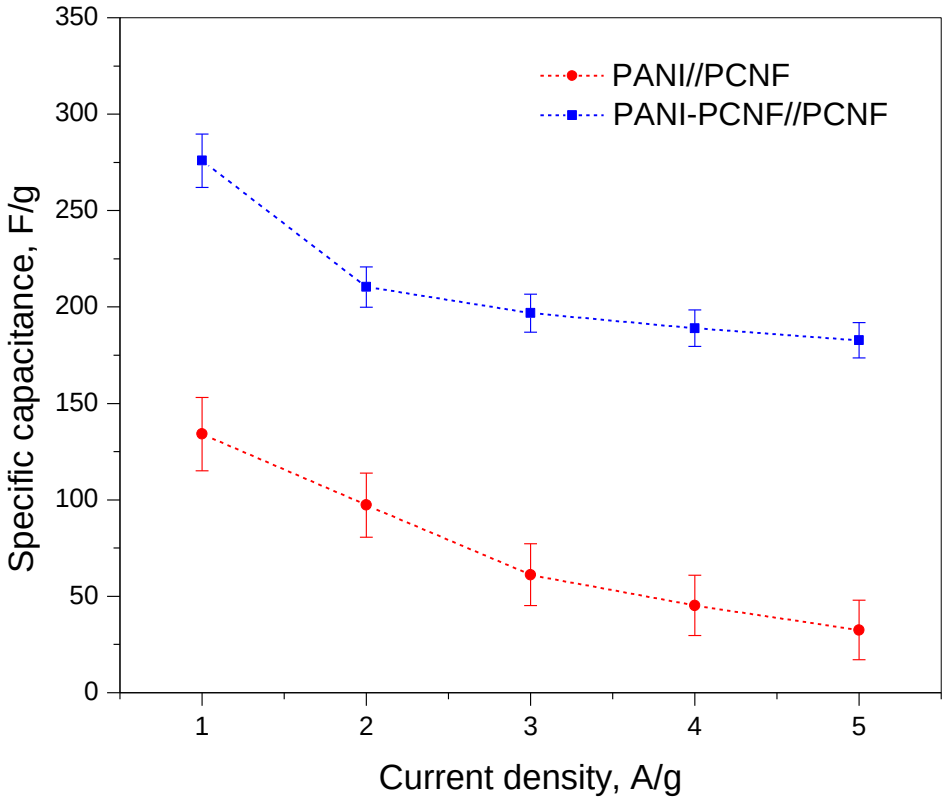

Figure 13. Specific capacitances of PANI//PCNF and PANI-PCNF//PCNF asymmetric supercapacitors.

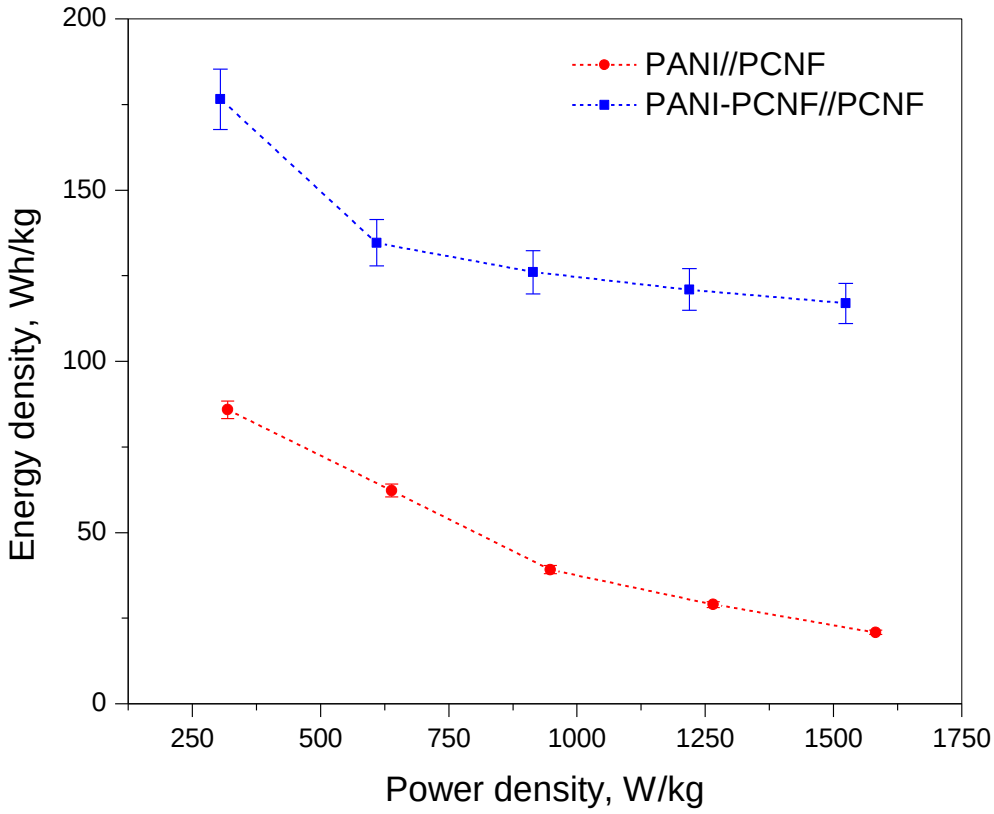

Figure 14. Ragone plots of PANI//PCNF, and PANI-PCNF//PCNF asymmetric supercapacitors.